Supplemental Information

Tropospheric Ozone Precursors: Global and Regional Distributions, Trends, and Variability

Yasin Elshorbany[1], Jerald R. Ziemke[2], Sarah Strode[2,3], Hervé Petetin[4], Kazuyuki Miyazaki[5], Isabelle De Smedt[6], Kenneth Pickering[7], Rodrigo J. Seguel[8], Helen Worden[9], Tamara Emmerichs[10], Domenico Taraborrelli[10], Maria Cazorla[11], Suvarna Fadnavis[12], Rebecca R. Buchholz[9], Benjamin Gaubert[9], Néstor Y. Rojas[13], Thiago Nogueira[14], Thérèse Salameh[15], Min Huang[16]

[1] School of Geosciences, College of Arts and Sciences, University of South Florida, St. Petersburg, FL, USA

[2] NASA Goddard Space Flight Center, Greenbelt, Maryland, USA

[3]Goddard Earth Sciences Technology and Research (GESTAR), Maryland, USA

[4]Earth Sciences Department, Barcelona Supercomputing Center, Barcelona, Spain

[5]Jet Propulsion Laboratory, California Institute of Technology, Pasadena CA

[6]BIRA-IASB, Ringlaan 3 Av. Circulaire, 1180 Brussels, Belgium

[7]Dept. of Atmospheric and Oceanic Science, University of Maryland, College Park, MD USA

[8]Center for Climate and Resilience Research, Department of Geophysics, Faculty of Physical and Mathematical Sciences University of Chile, Chile.

[9]Atmospheric Chemistry Observations and Modeling (ACOM), National Center for Atmospheric Research (NCAR), Boulder CO, USA.

[10]Institute of Energy and Climate Research, IEK-8: Troposphere, Forschungszentrum Jülich, Jülich, Germany.

[11]Universidad San Francisco de Quito USFQ, Instituto de Investigaciones Atmosféricas, Diego de Robles y Av Interoceánica, Quito, Ecuador.

[12]Center for Climate Change Research, Indian Institute of Tropical Meteorology, MoES, Pune, India.

[13]Department of Chemical and Environmental Engineering, Universidad Nacional de Colombia, Bogota, Colombia

[14]University of São Paulo, São Paulo, Brazil

[15]IMT Lille Douai, Institut Mines-Télécom, Univ. Lille, Centre for Energy and Environment, F-59000 Lille, France.

[16]University of Maryland, College Park, MD, USA

Table S 1: List of ozone sonde stations used in the study.

Station	Country or region	Latitude	Longitude	Source	Link
Alert	Canada	82.50	-62.30	HEGIFTOM	https://hegiftom.meteo.be/
Eureka	Canada	80.05	-86.42	HEGIFTOM	https://hegiftom.meteo.be/
Resolute	Canada	74.72	-97.98	HEGIFTOM	https://hegiftom.meteo.be/
Churchill	Canada	58.74	-94.07	HEGIFTOM	https://hegiftom.meteo.be/
Edmonton	Canada	53.55	-114.10	HEGIFTOM	https://hegiftom.meteo.be/
Goose Bay	Canada	53.30	-60.39	HEGIFTOM	https://hegiftom.meteo.be/
Legionowo	Poland	52.40	20.97	HEGIFTOM	https://hegiftom.meteo.be/
De Bilt	Netherlands	52.10	5.18	HEGIFTOM	https://hegiftom.meteo.be/
Uccle	Belgium	50.80	4.36	HEGIFTOM	https://hegiftom.meteo.be/
Kelowna	Canada	49.93	-119.40	HEGIFTOM	https://hegiftom.meteo.be/
Payerne	Switzerland	46.81	6.94	HEGIFTOM	https://hegiftom.meteo.be/
Yarmouth	Canada	43.87	-66.11	HEGIFTOM	https://hegiftom.meteo.be/
Madrid	Spain	40.45	-3.72	HEGIFTOM	https://hegiftom.meteo.be/
Izaña	Spain	28.30	-16.48	HEGIFTOM	https://hegiftom.meteo.be/
Paramaribo	Suriname	5.81	-55.21	HEGIFTOM	https://hegiftom.meteo.be/
Lauder	New Zealand	-45.04	169.68	HEGIFTOM	https://hegiftom.meteo.be/
Ny-Ålesund	Norway	78.91	11.88	NDACC	https://www-air.larc.nasa.gov/missions/ndacc/data.html
Thule	Greenland	76.53	-68.74	NDACC	https://www-air.larc.nasa.gov/missions/ndacc/data.html
Scoresbysund	Greenland	70.48	-21.97	NDACC	https://www-air.larc.nasa.gov/missions/ndacc/data.html
Sodankylä	Finland	67.37	26.65	NDACC	https://www-air.larc.nasa.gov/missions/ndacc/data.html
Haute Provence	France	43.94	5.71	NDACC	https://www-air.larc.nasa.gov/missions/ndacc/data.html
Dumont d'Urville	Antarctica	-66.67	140.00	NDACC	https://www-air.larc.nasa.gov/missions/ndacc/data.html
Neumayer	Antarctica	-70.65	-8.25	NDACC	https://www-air.larc.nasa.gov/missions/ndacc/data.html
McMurdo	Antarctica	-77.85	166.67	NDACC	https://www-air.larc.nasa.gov/missions/ndacc/data.html
Belgrano	Antarctica	-77.87	-34.62	NDACC	https://www-air.larc.nasa.gov/missions/ndacc/data.html

Summit	Greenland	72.34	-38.29	NOAA	ftp://ftp.gml.noaa.gov/data/ozwv/Ozonesonde/
Trinidad Head	United States	40.80	-124.16	NOAA	ftp://ftp.gml.noaa.gov/data/ozwv/Ozonesonde/
Boulder ESRL HQ (CO)	United States	39.99	-105.26	NOAA	ftp://ftp.gml.noaa.gov/data/ozwv/Ozonesonde/
Huntsville	United States	34.72	-86.64	NOAA	ftp://ftp.gml.noaa.gov/data/ozwv/Ozonesonde/
South Pole	Antarctica	-90.00	-169.00	NOAA	ftp://ftp.gml.noaa.gov/data/ozwv/Ozonesonde/
Wallops Island	United States	37.93	-75.47	SHADOZ	https://tropo.gsfc.nasa.gov/shadoz/Archive.html
Hanoi	Vietnam	21.01	105.80	SHADOZ	https://tropo.gsfc.nasa.gov/shadoz/Archive.html
Hilo (HI)	Northeastern Pacific	19.58	-155.07	SHADOZ	https://tropo.gsfc.nasa.gov/shadoz/Archive.html
Costa Rica	Costa Rica	9.94	-84.04	SHADOZ	https://tropo.gsfc.nasa.gov/shadoz/Archive.html
Kuala Lumpur	Malaysia	2.73	101.27	SHADOZ	https://tropo.gsfc.nasa.gov/shadoz/Archive.html
San Cristobal	Galapagos	-0.92	-89.62	SHADOZ	https://tropo.gsfc.nasa.gov/shadoz/Archive.html
Nairobi	Kenya	-1.30	36.75	SHADOZ	https://tropo.gsfc.nasa.gov/shadoz/Archive.html
Natal	Brazil	-6.00	-35.20	SHADOZ	https://tropo.gsfc.nasa.gov/shadoz/Archive.html
Watukosek	Java	-7.50	112.60	SHADOZ	https://tropo.gsfc.nasa.gov/shadoz/Archive.html
Ascension	South Atlantic	-7.58	-14.24	SHADOZ	https://tropo.gsfc.nasa.gov/shadoz/Archive.html
Samoa (Cape Matatula)	Southeastern Pacific	-14.25	-170.56	SHADOZ	https://tropo.gsfc.nasa.gov/shadoz/Archive.html
Fiji	South Pacific	-18.13	178.40	SHADOZ	https://tropo.gsfc.nasa.gov/shadoz/Archive.html
La Réunion	Southwestern Indian Ocean	-21.08	55.38	SHADOZ	https://tropo.gsfc.nasa.gov/shadoz/Archive.html
Irene	South Africa	-25.90	28.22	SHADOZ	https://tropo.gsfc.nasa.gov/shadoz/Archive.html
Idabel	United States	33.90	-94.75	TOPP	http://www.ruf.rice.edu/%7Eozone/
Houston	United States	29.72	-95.34	TOPP	http://www.ruf.rice.edu/%7Eozone/

Quito	Ecuador	-0.20	-78.44	USFQ	https://observaciones-iia.usfq.edu.ec/
Lerwick	United Kingdom	60.13	-1.10	WOUDC	https://woudc.org/data/explore.php?lang=en
Lindenberg	Germany	52.21	14.12	WOUDC	https://woudc.org/data/explore.php?lang=en
Valentia	Ireland	51.94	-10.25	WOUDC	https://woudc.org/data/explore.php?lang=en
Prague	Czech Republic	50.01	14.45	WOUDC	https://woudc.org/data/explore.php?lang=en
Hohenpeissenber g	Germany	47.80	11.01	WOUDC	https://woudc.org/data/explore.php?lang=en
Sapporo	Japan	43.06	141.33	WOUDC	https://woudc.org/data/explore.php?lang=en
Tateno (Tsukuba)	Japan	36.10	140.13	WOUDC	https://woudc.org/data/explore.php?lang=en
Naha	Japan	26.20	127.68	WOUDC	https://woudc.org/data/explore.php?lang=en
Hong Kong	China	22.31	114.17	WOUDC	https://woudc.org/data/explore.php?lang=en
Broadmeadows	Australia	-37.69	144.95	WOUDC	https://woudc.org/data/explore.php?lang=en
Macquarie Island	Australia	-54.50	158.94	WOUDC	https://woudc.org/data/explore.php?lang=en
Marambio	Antarctica	-64.24	-56.62	WOUDC	https://woudc.org/data/explore.php?lang=en
Davis	Australia	-68.58	77.97	WOUDC	https://woudc.org/data/explore.php?lang=en
Syowa	Antarctica	-69.00	39.58	WOUDC	https://woudc.org/data/explore.php?lang=en

CO MOPITT and CAM-chem simulation:

We compare simulations made by the Community Atmosphere Model with chemistry (CAM-chem) of the Community Earth System Model (CESM) version 2.1. The model is run at nominal 1°x1°, with comprehensive tropospheric and stratospheric chemistry, and includes nudging to the MERRA-2 reanalysis (Danabasoglu et al., 2020; Emmons et al., 2020). A baseline simulation uses the daily Quick-Fire Emissions Dataset (QFED) and monthly anthropogenic inventory from CAMS-GLOB-ANTv5.1 (Soulié et al., 2023). The anthropogenic CO emissions were replaced by the Community Emissions Data System version 2 or CEDSv2 (McDuffie et al., 2020).

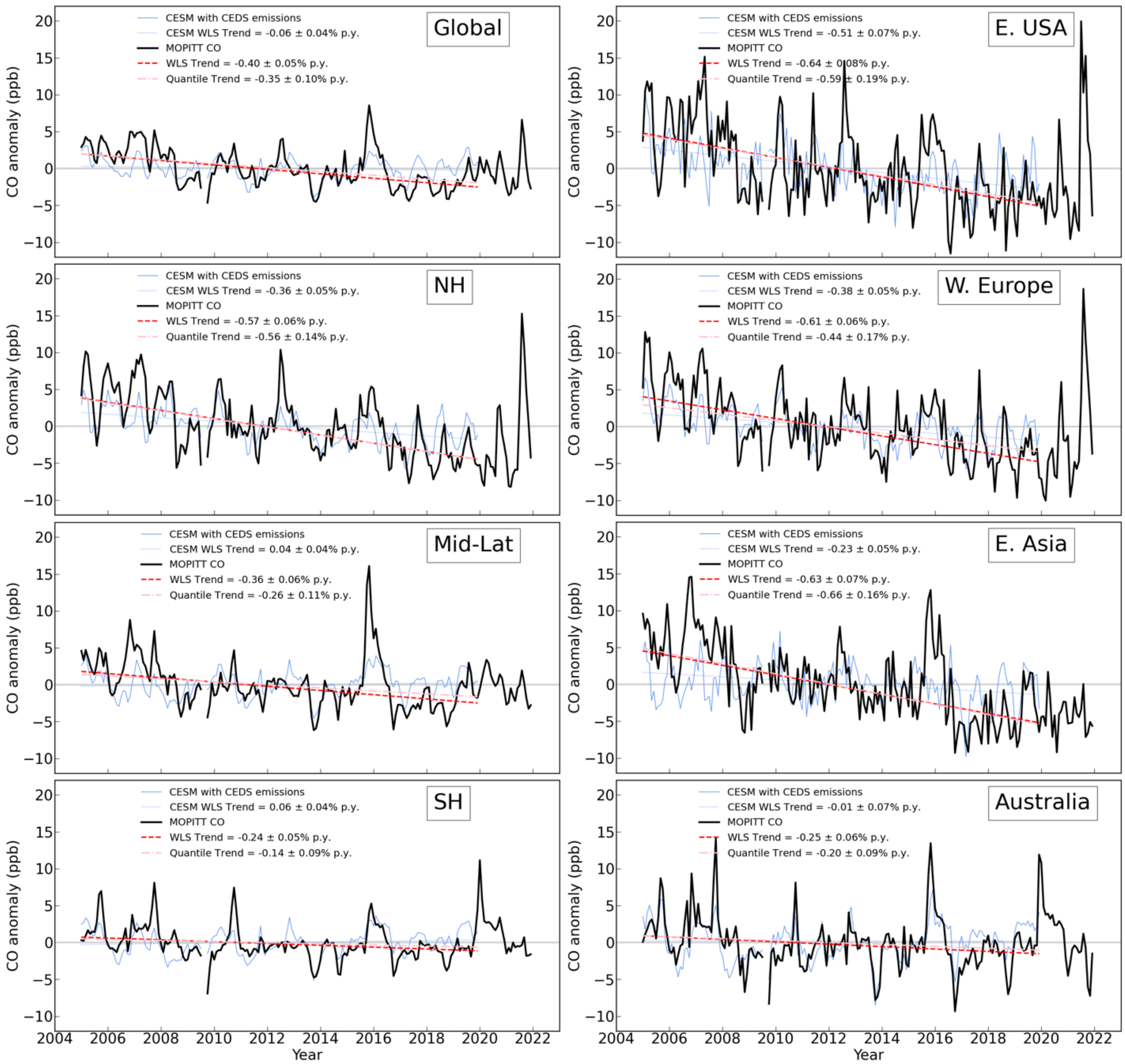

Figure S 1: MOPITT monthly average CO anomalies in column average volume mixing ratio (VMR), 2005-2021 (black). Updated dataset based on Buchholz et al. (2021). Data is Level 3, monthly average daytime observations, using version 9 joint NIR/TIR retrievals. Regions are defined in Figures 10 and 11. Trends are calculated on anomalies 2005-2019. The weighted Least Squares trend (red) is weighted by the monthly regional standard deviation. The quantile regression trend is also shown (pink). The quantile regression trend is also shown (pink). Grey line indicates zero. CESM simulation results are shown as a comparison. Model output was convolved with the MOPITT averaging kernel prior to calculating regional month average CO anomalies (blue solid line) and WLS trends (blue dotted line).

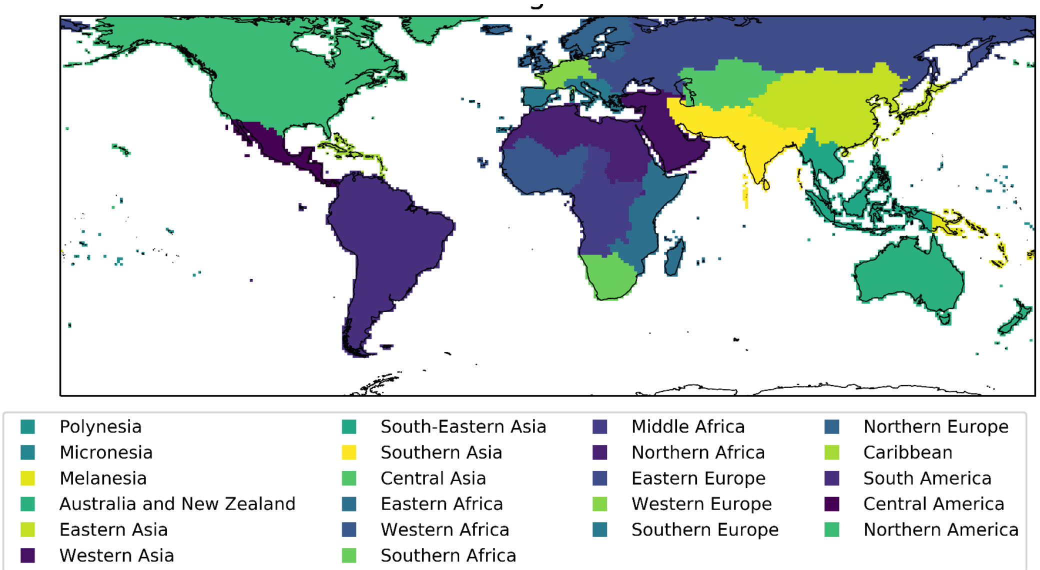

Figure S 2: Map of the regions used for computing the regional OMI QA4ECV TrC-NO_2 and TrC-HCHO trends.

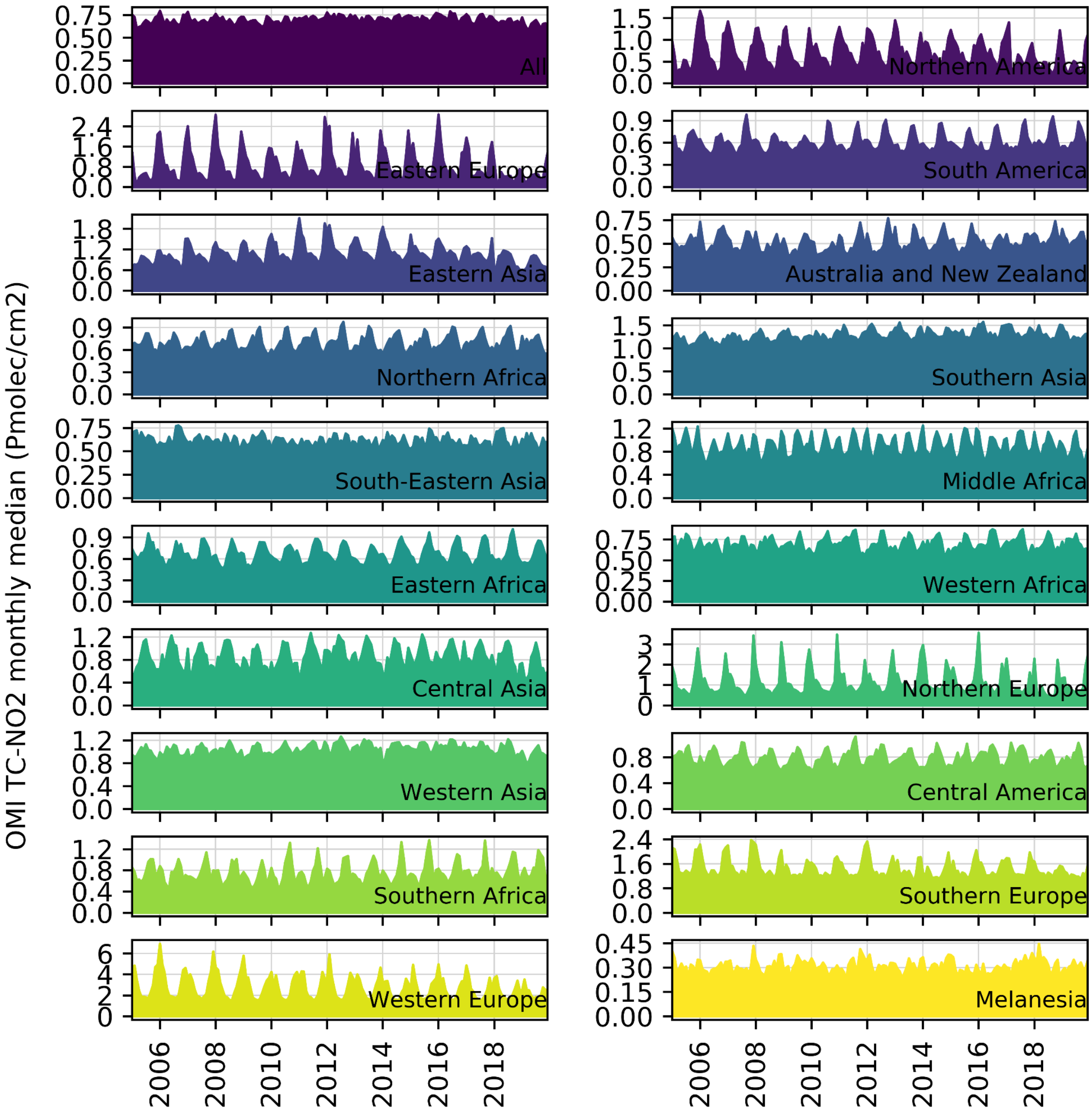

Figure S 3: Monthly regional time series of OMI QA4ECV TrC-NO2.

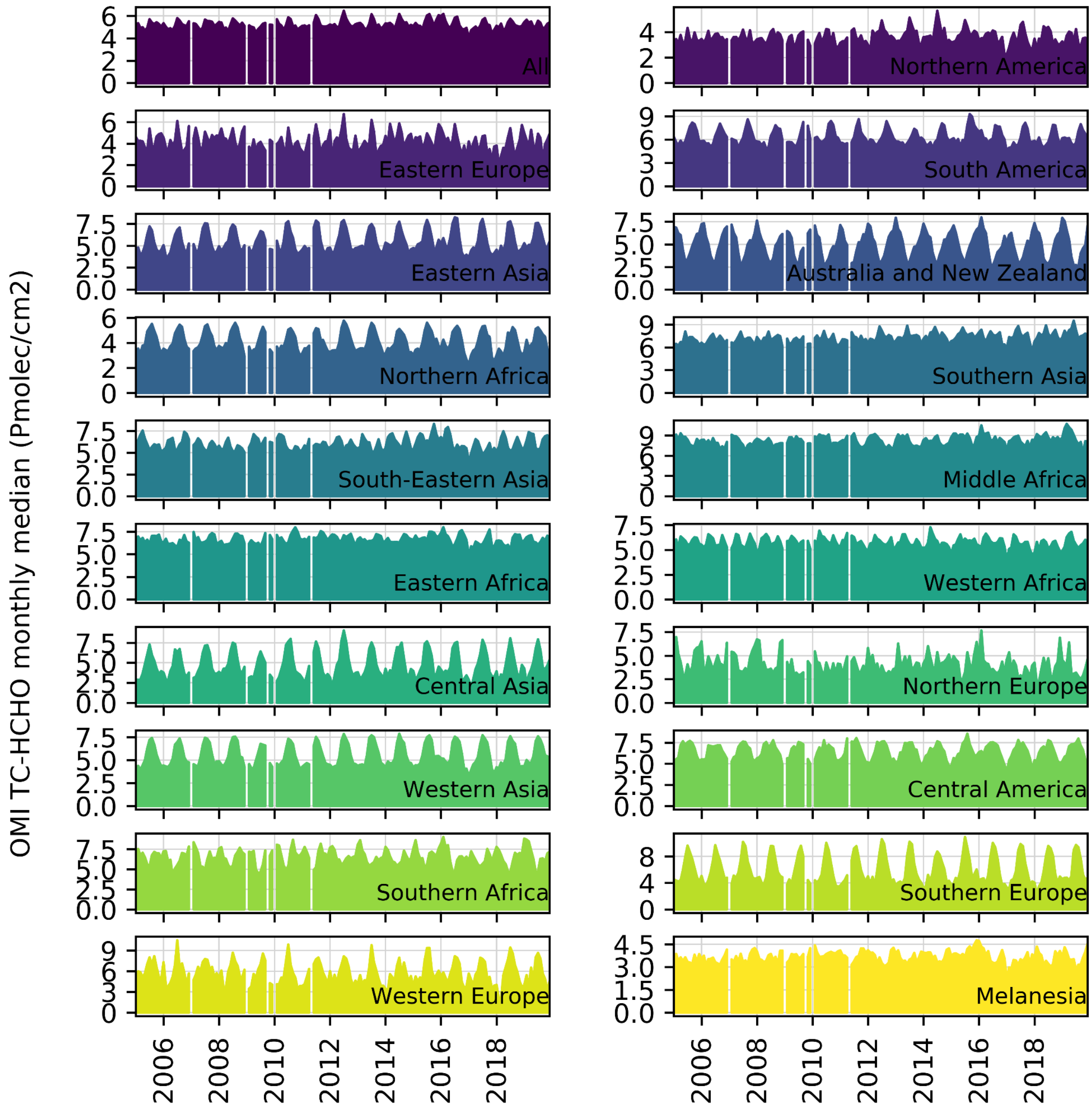

Figure S 4: Monthly regional time series of OMI QA4ECV TrC-HCHO.

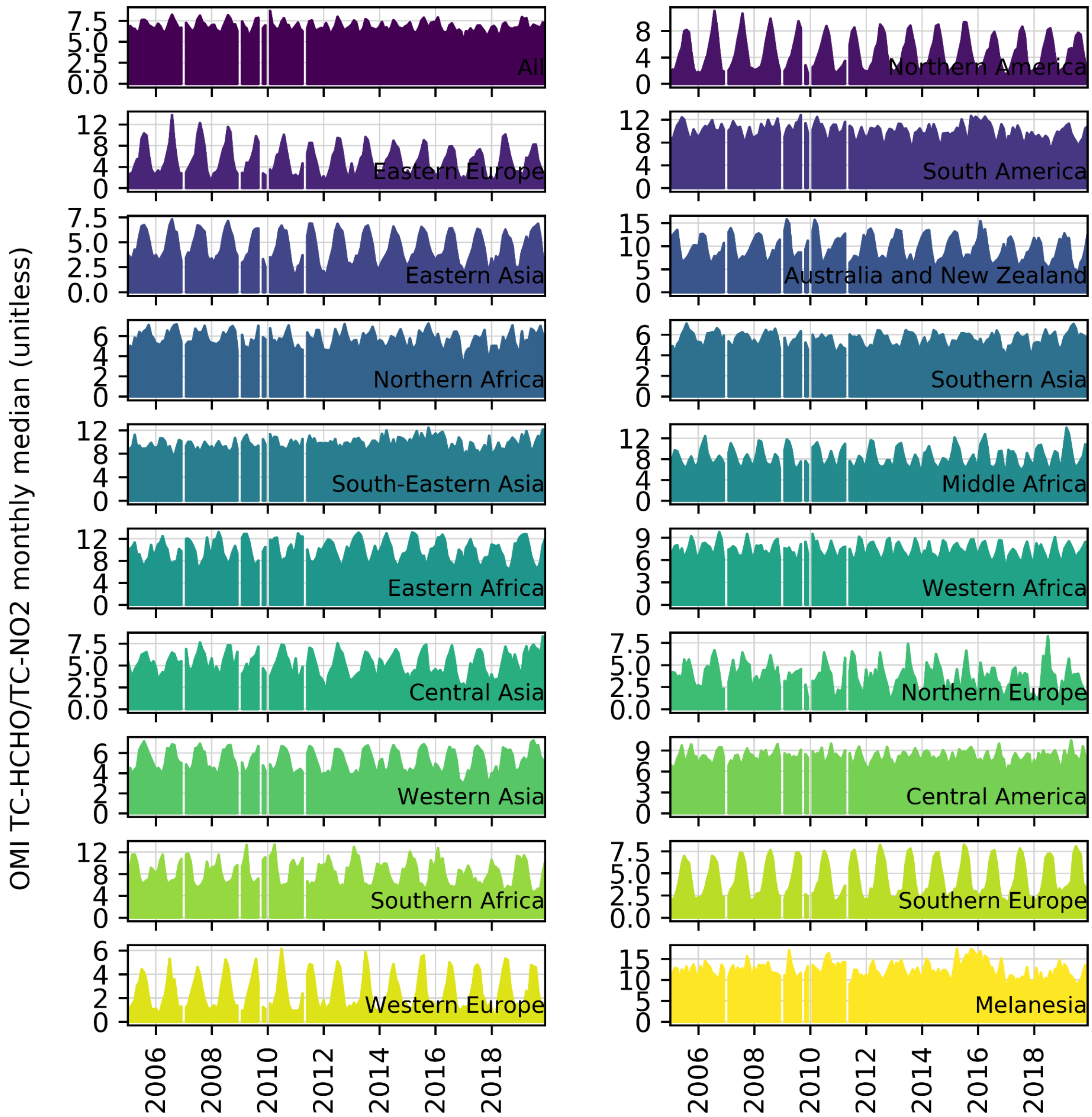

Figure S 5: Monthly regional time series of OMI QA4ECV TrC-HCHO/NO2.